Effect of soft flares on XMM-Newton EPIC-pn timing mode data

Vadim Burwitz[a], Frank Haberl[a], Michael Freyberg[a], Konrad Dennerl[a],
Eckhardt Kendziorra[b], Markus Kirsch[c]
[a] Max-Planck-Institut für extraterrestrische Physik, Giessenbachstr. , D-85748 Garching, Germany
[b]Institut für Astronomie und Astrophysik, Eberhard-Karls-Universität, D-72026 Tübingen, Germany
[c]XMM-Newton Science Operations Center/VILSPA,Spain

ABSTRACT

The EPIC-pn CCD Camera on board the ESA X-ray observatory XMM-Newton is a very sensitive and versatile instrument with many observing modes. One of the modes, the timing mode, was designed so that a time resolution of 0.029 milliseconds can be achieved. This mode is important for observing bright variable sources with a very high time resolution. Up to now the it has only been possible to use the spectra down to 300-400 eV in this mode. Below this energy the data appears to be affected by soft flares which are caused by stack overflows generated by high energy particles. We present a method that can be used to mitigate the effect these flares have on the data and discuss the improvement that this brings to the timing mode spectra. This new method will at last make it possible to get spectra down to the lowest energies detectable in this mode. This is particularly interesting for timing studies of isolated neutron stars and other variable objects, such as magnetic CVs, with very soft spectra.

Keywords: XMM-Newton, pn-CCD, X-ray detectors, X-ray calibration, Timing

1. INTRODUCTION

Among the many instruments on board the XMM-Newton X-ray observatory[1], the pn-CCD detector[2,3] of the European Photon Imaging Cameras (EPIC)[4] has data read out modes which allow timing observations to be performed with a time resolution from 283 msec in the extended full-frame down to 6 μsec in the burst mode. Compared to other X-ray CCD systems currently used in astrophysics the pn-CCD is the X-ray CCD camera with the fastest readout available at the moment. Fast read-out CCDs are needed for two reasons: the first to obtain data with a sufficiently high time sampling to study the astrophysical object inherent short time scales such as the physics of the accretion onto neutron stars and black holes in X-ray binaries, the second in the case of bright objects to avoid the true shape of their spectra to be changed by pile-up (i.e. when two photons arriving at the same position in the same frame are read out as one). Not only galactic X-ray binaries are bright but also extragalactic objects such as quasars. The mode usually used for analyzing these kinds of objects is the timing mode which has a time resolution of 29.6 μsec. Compared to other timing missions such a RXTE[i], the pn-CCD has a high spectral resolution over a broad energy range 0.1-12 keV including the especially the interesting range from 0.1-2 keV not covered by RXTE.

After launch the pn-CCD timing mode showed a much higher than expected background at low energies < 0.25 keV. This problem was revealed during the analysis of several of the timing mode observations of objects with soft spectra thus sparking the need to find out the cause and a solution to the problem. In §2 we describe the data sets used for this analysis, in §3 we describe the methods used for analyzing the data, and finally in §4 we discuss the results.

2. XMM-NEWTON DATA

A total of 9 XMM Newton pn-CCD camera datasets obtained in timing mode were used in the following analysis (see Table 1). All the data where processed using XMM-Newton SAS[ii] version 5.4.1. with the high energy cutoff threshold disabled (all events with PHA < 4096) so that a possible correlation between MIPS and soft X-ray flares can be searched for in this analysis. These datasets were chosen so that one can study these soft flares at high and low count rates. Also the cal closed observations were used to find out if the soft flares are present in that data.

[i] http://heasarc.gsfc.nasa.gov/docs/xte
[ii] XMM-Newton Science Analysis Software, http://xmm.vilspa.esa.es/external/xmm_sw_cal/sas.shtml

X-Ray and Gamma-Ray Instrumentation for Astronomy XIII, edited by Kathryn A. Flanagan,
Oswald H. W. Siegmund, Proceedings of SPIE Vol. 5165 (SPIE, Bellingham, WA, 2004)
0277-786X/04/$15 · doi: 10.1117/12.506363

Table 1: List of XMM-Newton EPIC-pn CCD timing mode observations used for the analysis

Object	Orbit	Observation number	Mode	Filter	Exposure [Sec]	Obs. Start UT	Obs. End UT
Cal. closed	0136	0101441001 PNS003	FT	Closed	18021	2000-09-04 21:02:07	2000-09-05 02:02:28
XB1254-69	0206	0060740101 PNS003	FT	Thin1	15219	2001-01-22 15:49:19	2001-01-22 20:02:58
Her X-1	0207	0134120101 PNS005	FT	Medium	9274	2001-01-26 01:27:08	2001-01-26 04:01:42
PKS2155-304	0362	0124930301 PNS025	FT	Medium	44304	2001-11-30 03:12:05	2001-11-30 15:30:29
Crab	0411	0153750401 PNS001	FT	Thick	9034	2002-03-08 10:03:49	2002-03-08 12:34:23
PKS2155-304	0545	0124930601 PNS021	FT	Thick	55045	2002-11-30 15:57:29	2002-12-01 07:14:54
Mkn421	0546	0136541001 PNS008	FT	Medium	69913	2002-12-01 23:18:35	2002-12-02 18:43:48
V4743Sgr	0608	0127720501 PNU014	FT	Thin1	30041	2003-04-04 23:44:58	2003-04-05 08:05:39
Cal.closed	0644	0125321001 PNS010	FT	Closed	12790	2003-06-15 08:44:58	2003-06-15 12:18:08

3. ANALYSIS OF THE SOFT FLARES IN THE TIMING MODE DATA

The analysis of the data was done in several steps: first of all the difference in arrival time between consecutive photons Δt was computed at each time t in order to determine whether there are any gaps in the data that are not caused by the observed source but can be attributed to instrumental effects. In an ideal world this $1/\Delta t$ would correspond to the source count rate. In the case of the datasets described in Table 1 we find that there are gaps present in the data that correspond to different effects in the on-chip and on-board electronics each with their characteristic timescales. In Fig. 1 an example of Δt's versus t for the EPIC pn-CCD observation of the X-ray binary Hercules X-1 is shown. Three different gap sizes are apparent in all the observations with high count rates. Due to the limited telemetry bandwidth of the X-ray observatory it can happen that more photons are processed on-board than can be transmitted to the ground station so that when the transmission buffer is reset, gaps with a typical length of ~22 sec appear at regular intervals in the data. This happens when the total measured count rate is greater than ~300 counts/sec. On the other hand if the count rate exceeds more than ~2000 counts/sec the electronics can be saturated and the FIFO buffer is automatically reset which also causes additional gaps in the data. These gaps are shorter, of the order of ~0.1 sec. This analysis was done because in the beginning we noticed that the brighter soft X-ray flares generate FIFO gaps (see Fig. 2) and we wanted to check whether the are any other effects to take in to account.

Before actually proceeding to remove the soft X-ray flares much effort was put into finding out where they are generated on the CCD chip, whether they are localized, or appear at different places, whether they are always present no matter if an object is being observed or not. Figures 3 and 4 respectively help answer these questions. The former shows that these flares are also present even though there is no X-ray light from the telescopes passing through to the CCD detector. So the likely cause for such soft flares is very high energy particles that generate such a bright energetic tail that the electronics detect it as pseudo low energy events i.e. the flares we see. The latter Figure also shows that even though an object is being observed, the soft flares can occur anywhere on the CCD chip. A detailed analysis of the bottom parts of the plots in Figures 3 and 4 and similar plots for other objects indicate that the flares can happen at any point on the detector and that MIPS are not necessarily always detected close to the start of a flare trail.

Finally an algorithm to remove the flares was developed so that also flares which have generated a FIFO gap can be removed. This is done by smoothing the binned < 0.25 keV light curve so that a threshold can be set that the regions in the light curve containing flares can be flagged and then removed from the light curve. The results of the application of this method to the EPIC pn-CCD observation of the X-ray binary Hercules X-1 are shown in Figure 5.

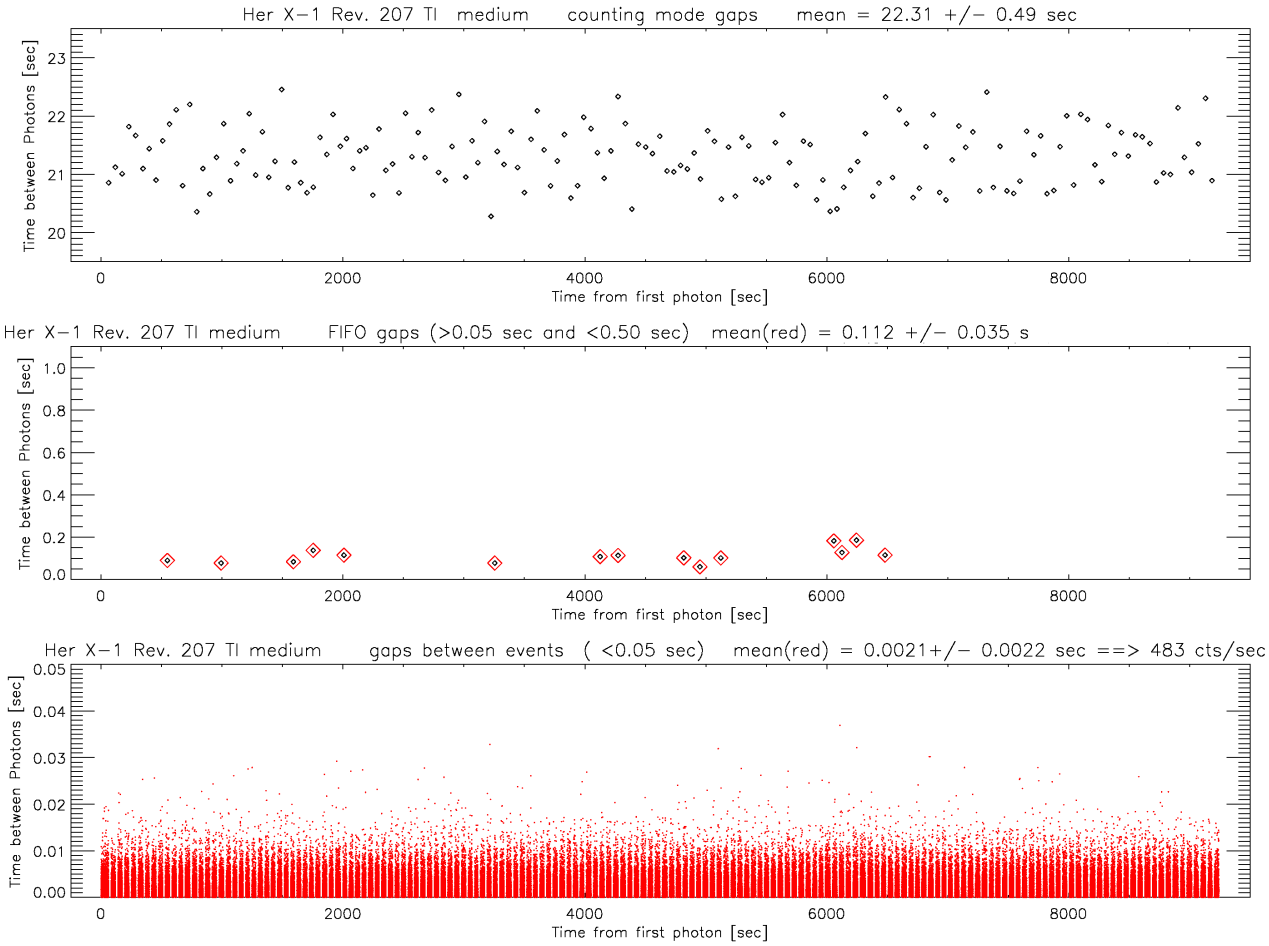

Figure 1: Plot showing the time between consecutive photons Δt versus time t for the complete EPIC pn-CCD observation in orbit 0207 of the X-ray binary Hercules X-1. The panels from top and bottom show the different Δt's present in the observation. The bottom panel shows the Δt's due to the source count rate, the central panel shows the typical FIFO overflow Δt's caused by on the CCD electronics not being able to handle the extremely high count rate and the top panel shows the counting mode Δt's due to telemetry saturation.

At the time of writing this screening method is being improved and made more robust so that it can be applied to any dataset without lots of manual intervention to optimize thresholds. This will be part of a software tool that will be included in the XMM-Newton SAS.

4. CONCLUSIONS

Our analysis of the different datasets (see Table 1) with the methods described in section 3 shows that it is a well spent effort to remove the soft X-ray flares from the data in order to obtain spectra down to the lowest energies detectable in this mode i.e. 0.2 keV (again see the corrected spectrum in Fig. 5). This is particularly interesting for timing studies of isolated neutron stars and other variable objects, such as magnetic CVs, which have very soft spectra as well as for neutron star and black hole X-ray Binaries and Quasars which also have in some cases a pronounced soft component.

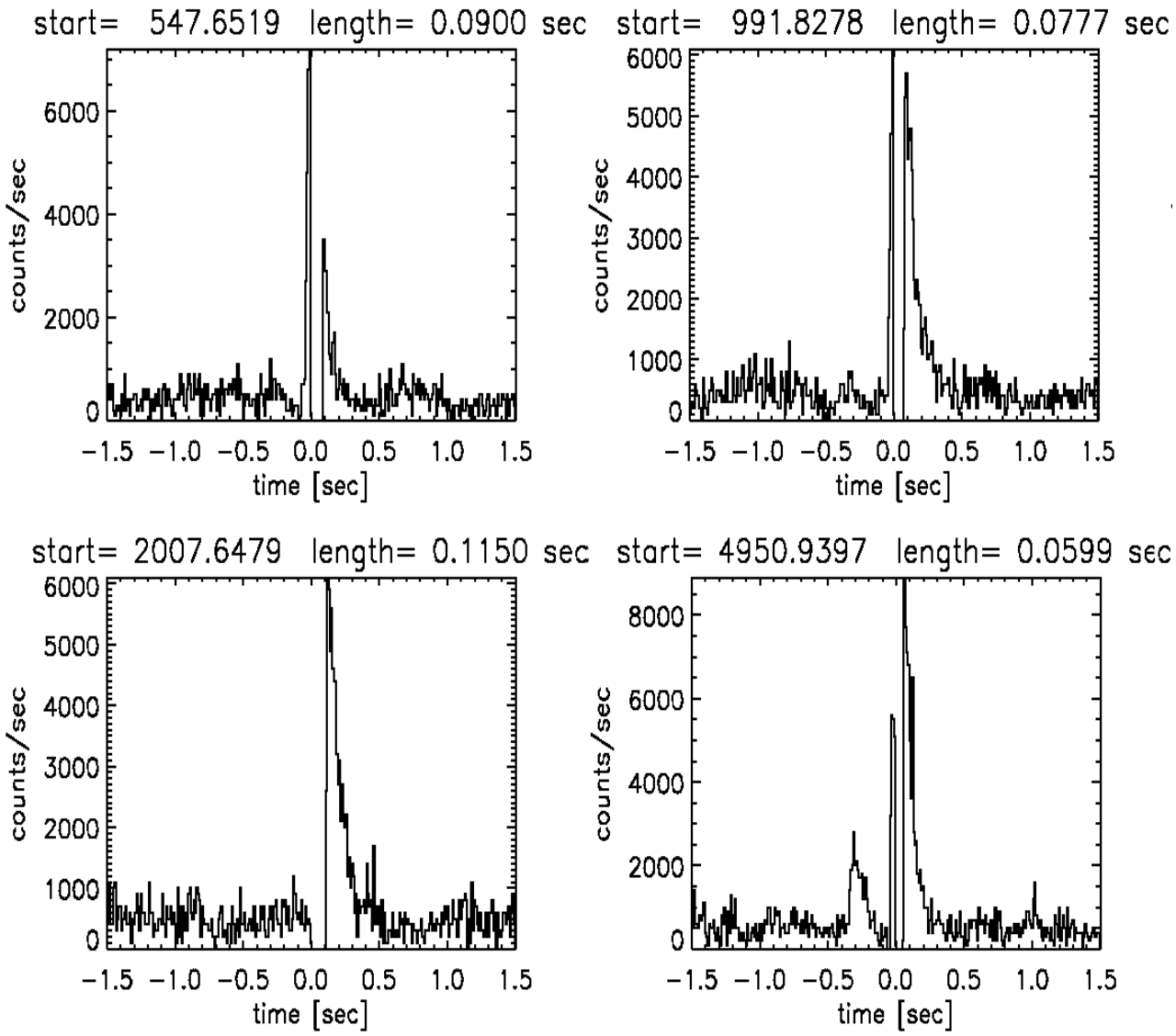

Figure 2: Plot showing 4 soft X-ray flares around FIFO gaps in the EPIC pn-CCD observation in orbit 0207 of the X-ray binary Hercules X-1. These 4 graphs depict the high count rates that can appear in some of the flares and how they can be directly associated with the generation of FIFO gaps. The bottom right panel shows at t=-0.4 that there are also smaller but still bright flares that do not generate FIFO gaps.

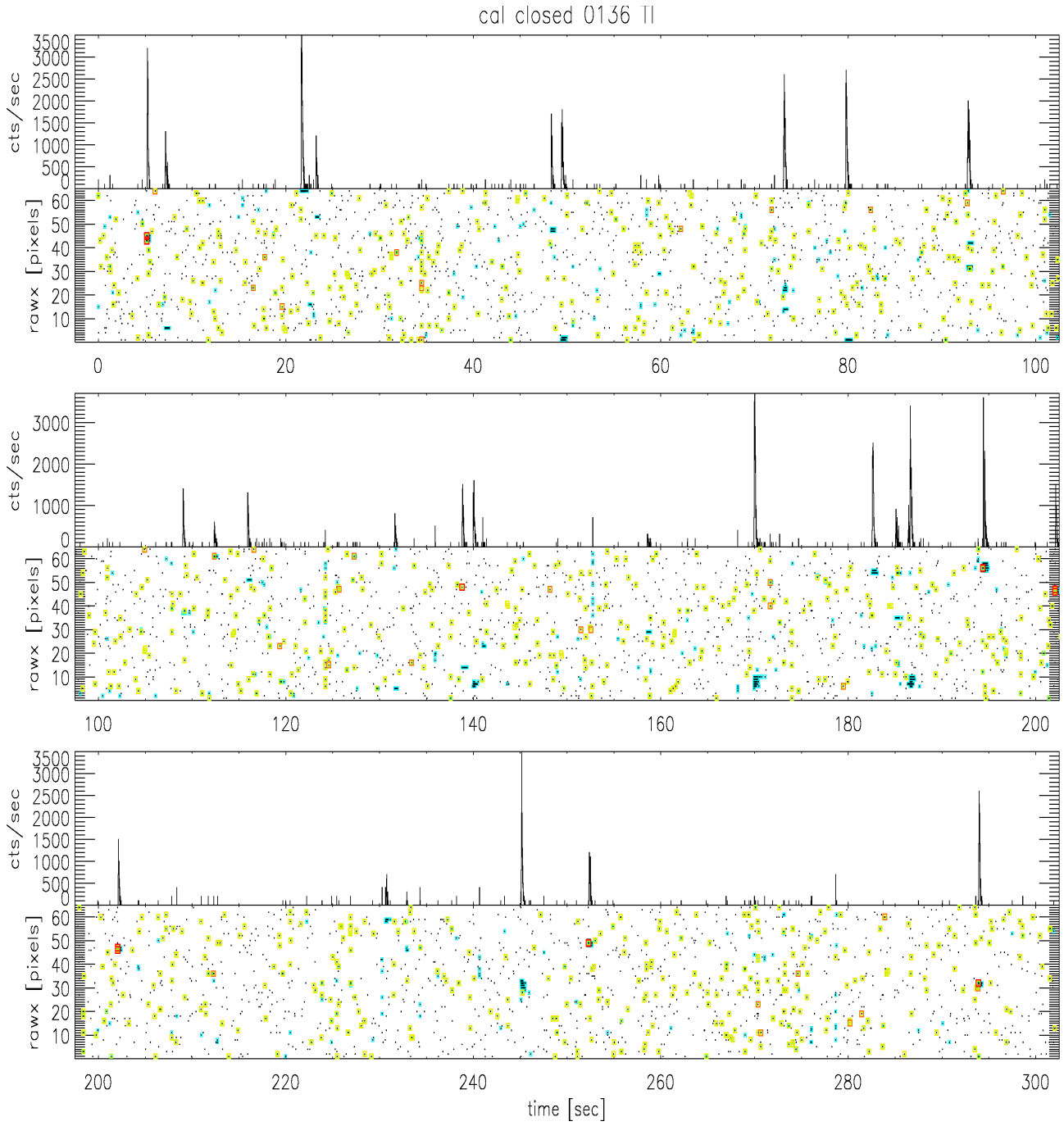

Figure 3: Plot showing the first 300 seconds of the EPIC pn-CCD cal-closed observation in orbit 0136. The 3 panels here each show 100 seconds of data. The top of each panels shows the X-ray light curve, count rate versus time with detected counts in the 0.20-0.25 keV X-ray band. The bottom part of each panel shows the time evolution and location of individual flare events in format RAW X (which corresponds to the CCD column) vs. time. Here the dark splotches which correspond to the flares above, show that these are not point like but usually spread out over one or more columns depending on the intensity. All detected events are displayed as a dot. Events with a thick square around them have a value for the PHA > 3500 corresponding to high energy MIPS. The total count rate for this cal-closed observation is very low as no sky photons can reach the detector.

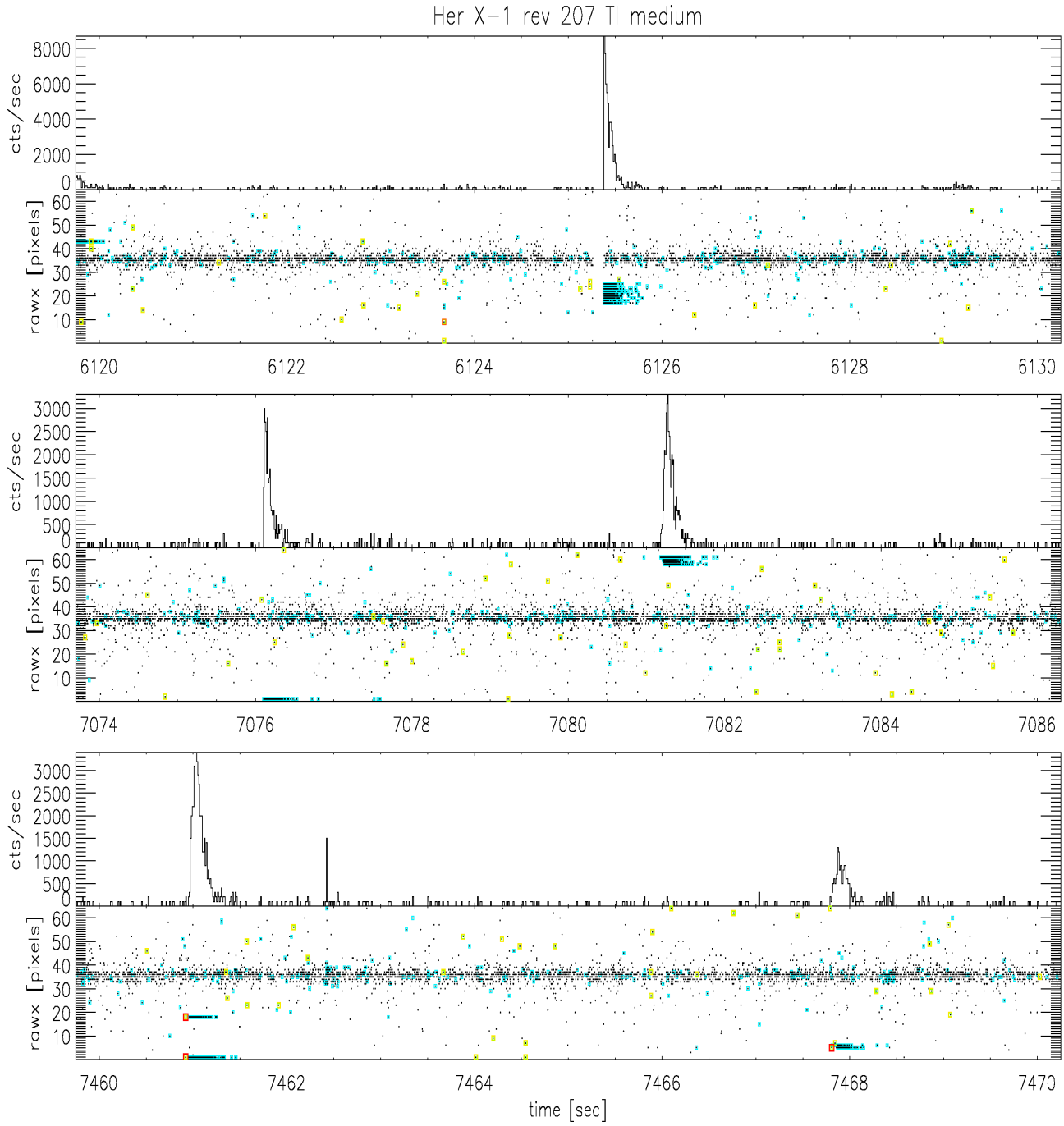

Figure 4: Plot with 3 panels each showing a 12 second piece of the EPIC pn-CCD observation in orbit 0207 of the X-ray binary Hercules X-1. The top of each panels shows the X-ray light curve, count rate versus time with detected counts in the 0.20-0.25 keV X-ray band. The bottom part of each panel shows the time evolution and location of individual flare events in format RAW X (which corresponds to the CCD column) vs. time. Here the dark splotches which correspond to the flares above, showing that these are not point like but usually spread out over one or more columns depending on the intensity. All detected events are displayed as a dot. Events with a thick square around them have a value for the PHA > 3500 corresponding to high energy MIPS. In this figure the dark line with a concentration of photons corresponds to the source. In the top panel of this observation one can clearly see a FIFO gap.

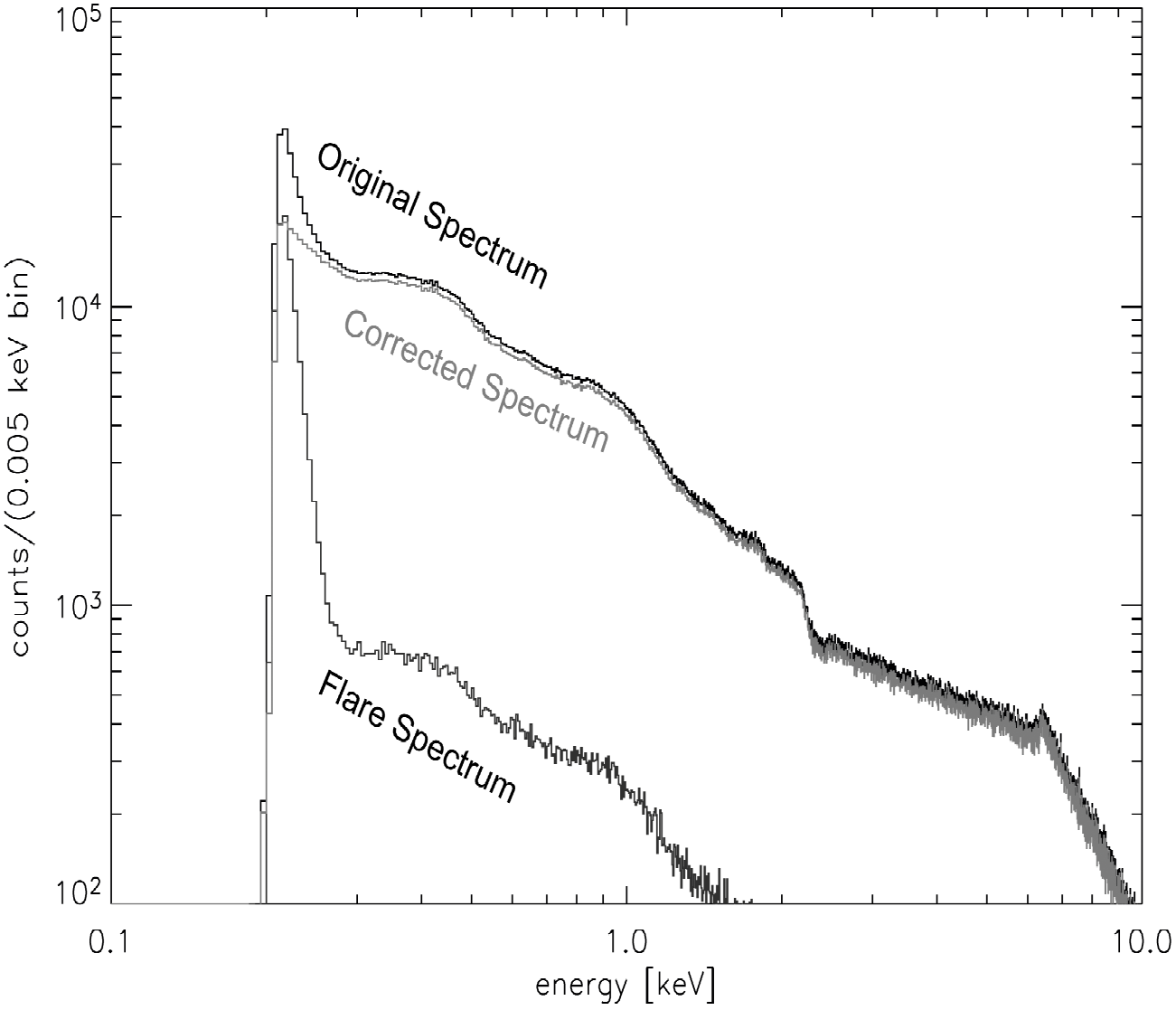

Figure 5: Plot showing the spectra for using only singles of observation in orbit 0207 of the X-ray binary Hercules X-1. The top curve shows the spectrum without corrections for flares. Just below the spectrum is shown that one obtains after subtracting the flare spectrum (plotted below the other two spectra) with a strong peak. This clearly shows that this screening method has the desired effect of allowing the spectral data to be used down to lowest energies.

5. REFERENCES

1. F. Jansen, D. Lumb, B. Altieri, J . Clavel, M. Ehle, et al., "XMM-Newton Observatory. I. The spacecraft and operations," A&A 365, pp. Ll-L6, Jan. 2001.

2. L. Strüder, N. Meidinger, E. Pfeffermann, R. Hartmann, H. W. Brauninger, et al., "X-ray pn-CCDs on the XMM Newton Observatory," in Proc. SPIE, X-Ray Optics, Instruments, and Missions 111, Joachim E. Trümper; Bernd Aschenbach; Eds., 4012, pp. 342-352, July 2000.

3. L. Strüder, U. Briel, K. Dennerl, R. Hartmann, E. Kendziorra, et al., "The European Photon Imaging Camera on XMM-Newton: The pn-CCD camera," A&A 365, pp. L18-L26, Jan. 2001.

4. G. E. Villa, A. F. Abbey, M. Arnaud, M. Balasini, G. F. Bignami, et al., "The EPIC system onboard the ESA XMM mission," in Proc. SPIE Vol. 2808, p . 402-413, EUV, X-Ray, and Gamma-Ray Instrumentation for Astronomy VII, Oswald H. Siegmund; Mark A. Gummin; Eds., pp. 402-413, Oct. 1996.